

The Data Processing of the LAMOST Medium-Resolution Spectral Survey of Galactic Nebulae (LAMOST MRS-N Pipeline)

Chao-Jian Wu^{1,2}, Hong Wu^{1,2}, Wei Zhang^{1,2}, Yao Li^{2,3}, Juan-Juan Ren^{2,4}, Jian-Jun Chen^{1,2}, Chih-Hao Hsia⁵, Yu-Zhong Wu^{1,2}, Hui Zhu², Bin Li^{6,7}, Yong-Hui Hou^{3,8},

- ¹ CAS Key Laboratory of Optical Astronomy, National Astronomical Observatories, Chinese Academy of Sciences, Beijing 100101, China; chjwu@bao.ac.cn
- ² National Astronomical Observatories, Chinese Academy of Sciences, 20A Datun Road, Chaoyang District, Beijing 100101, China
- ³ School of Astronomy and Space Science, University of Chinese Academy of Sciences, Beijing 100049, China;
- ⁴ CAS Key Laboratory of Space Astronomy and Technology, National Astronomical Observatories, Chinese Academy of Sciences, Beijing 100101, China
- ⁵ State Key Laboratory of Lunar and Planetary Sciences, Macau University of Science and Technology, Taipa, Macau, China
- ⁶ Purple Mountain Observatory, Chinese Academy of Sciences, Nanjing 210008, People's Republic of China
- ⁷ University of Science and Technology of China, Hefei 230026, People's Republic of China
- ⁸ Nanjing Institute of Astronomical Optics, & Technology, National Astronomical Observatories, Chinese Academy of Sciences, Nanjing 210042, China

Received —; accepted —

Abstract The Large sky Area Multi-Object Fiber Spectroscopic Telescope (LAMOST) medium-resolution spectral survey of Galactic Nebulae (MRS-N) has conducted for three years since Sep. 2018 and observed more than 190 thousands nebular spectra and 20 thousands stellar spectra. However, there is not yet a data processing pipeline for nebular data. To significantly improve the accuracy of nebulae classification and their physical parameters, we developed the *MRS-N Pipeline*. This article presented in detail each data processing step of the *MRS-N Pipeline*, such as removing cosmic rays, merging single exposure, fitting sky light emission lines, subtracting skylight, wavelength recalibration, measuring nebular parameters, creating catalogs and packing spectra. Finally, a description of the data products, including nebular spectra files and parameter catalogs, is provided.

Key words: surveys — catalogs — methods: data analysis — ISM: general

1 INTRODUCTION

The LAMOST MRS-N, (Wu et al., 2020; Wu et al., 2021), as a sub-project of the Medium-Resolution Spectral Survey (MRS, (Liu et al., 2020)), mainly relies on the LAMOST (also known as Guoshoujing Telescope), which is the first astronomical large-scale scientific facility of China (Cui et al., 2012; Zhao et al., 2012; Wang et al., 1996; Su & Cui, 2004) and has achieved great success in many fields of astronomy (Liu et al., 2020; Gao et al., 2014; Liu et al., 2015; Karoff et al., 2016; Luo et al., 2016; Wang et al., 2017b; Ren et al., 2018b; Liu, 2019; Liu et al., 2019; Gu et al., 2019; Wu et al., 2016,

2020; Tian et al., 2015; Xiang et al., 2015a; Huang et al., 2016; Liu et al., 2017a,b; Tian et al., 2017; Wang et al., 2017a; Li et al., 2018; Tian et al., 2018; Wang et al., 2018; Xu et al., 2018; Yu & Liu, 2018; Zhao et al., 2018; Li et al., 2019; Tian et al., 2019; Wang et al., 2019b,a; Shen et al., 2016; Wu et al., 2010a,b; Huang et al., 2019), to observe the nebulae (including the H II regions, Herbig-Haro objects, supernova remnants, planetary nebulae) in the northern Galactic Plane (GP). From October 2018 to now, MRS-N has been conducted for three years and obtained more than 190 thousand medium resolution spectra of Galactic nebulae. It is one of the largest nebular survey in the world (Wu et al., 2021).

Several pipelines have been developed to reduce the LAMOST raw data. LAMOST 2D Pipeline (Luo et al., 2015) is used to extract spectra from CCD images, like subtracting dark and bias, correcting flat field, extracting spectra, calibrating wavelength, subtracting sky light, merging spectra, etc., and do flux calibration, while 1D Pipeline (Luo et al., 2015), which is used after 2D Pipeline, works on the classification and parameter measurement of stars, galaxies or quasars (QSOs). Xiang et al. (2015b) introduced the LAMOST stellar parameter pipeline at Peking University (LSP3), which is parallel to the LAMOST 1D Pipeline. The main function of LSP3 is to determinate the radial velocities (RVs) and stellar atmospheric parameters, such as T_{eff} , $\log g$ and $[\text{Fe}/\text{H}]$. However, the LAMOST 1D Pipeline and LSP3 are mainly used to measure stellar parameters. They are both not suitable for the data of MRS-N. A MRS-N spectrum contains dozens of strong sky light emission lines, nebular emission lines and faint continuum. Unlike the stellar spectra, it is difficult to reduce the sky light effectively. Especially in a large scale nebular region, it is very difficult to find the spectrum of pure sky light. In other words, the sky light of MRS-N data cannot be reduced with the regular method in the LAMOST 2D Pipeline. Specific algorithms are required. We first obtain the spectra (can be thought as the MRS-N raw data) that have been done wavelength calibration but have not been done the sky light subtraction by the LAMOST 2D Pipeline. Then we developed a new pipeline only for the MRS-N raw data, which is named ***MRS-N Pipeline***.

In this paper, we first introduce the MRS-N observation of past three years in Section 2. Section 3 describes merging single exposure, wavelength calibration, subtracting sky light and measuring nebular parameters in detail. The data products are presented in Section 4. Finally, Section 5 gives a brief summary.

2 OBSERVATION

From October 2018 to now, we have completed three years of MRS-N observation. The observations in the three years are from Oct. 2018 to Jan. 2019, Nov. 2019 to Mar. 2020 and Oct. 2020 to Mar. 2021, respectively. As described in Wu et al. (2021), MRS-N observation should be carried on at moonless time. Due to the weather and some irresistible reasons, only 9 days were suitable for observing and finally 12 plates were finished in the first year. We have optimized the observation strategy comparing with the first year, then we finished 31 plates. Among the 31 plates, 20 observed plates were covered into an united area included Rosette Nebula and NGC2264 (***Ros*** area; Wu et al. (2021)), 2 plates were covered in the Westerhout 5 area (***West***) and the left 9 were observed to cover the GP area. In the second year, we finished a complete specific area, the ***Ros*** area. In the third year, mainly due to the weather, the number of observed areas decreased. Only 11 days were suitable for observing and finally 17 plates were finished in the third year.

Figure 1 shows the three years coverage of MRS-N. The blue circles indicate observations of the first year, the green circles indicate the second year's observations and the red circles indicate the third year's observations. All the observed MRS-N data will be processed by using the pipeline described below.

3 METHODOLOGY

As described in Wu et al. (2021), the data processing of MRS-N is different from the stellar reduction, meaning that the LAMOST 1D pipeline (Luo et al., 2012, 2015) and LSP3 (Xiang et al., 2015b) are not suitable for MRS-N data. So we developed the ***MRS-N Pipeline***. The ***MRS-N Pipeline*** includes removing cosmic rays, merging single exposure, fitting skylight emission lines (Ren et al., 2021), subtracting

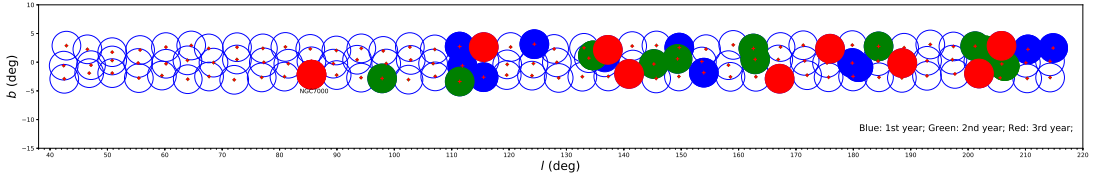


Fig. 1 MRS-N coverage of past three years' observation. The x-axis represents the longitude and the y-axis represents the latitude. The blue circles indicate observation of the first year, green and red circles indicate observations of the second and the third year, respectively.

skylight (Zhang et al., 2021), wavelength recalibration, parameters measurement of nebular emission lines, creating catalog and packing spectra. Figure 2 illustrates a flowchart of *MRS-N Pipeline*.

In addition to these main steps above, the *MRS-N Pipeline* can also update the fits (Flexible Image Transport System) header of spectral fits files and calibrate the science spectra without coordinates. *MRS-N Pipeline* obtained a linear relationship through the known coordinates and known pixel positions of the spectra. Using the relationship, the coordinates of those spectra with only pixel positions can be estimated. The purpose of this step is to improve the utilization of fibers.

3.1 Merging single exposure

A MRS-N plate contains 3 spectra with 900s exposure (called single exposure). The first step of *MRS-N Pipeline* is to coadd the 3 single exposure spectra. The main purpose of coadding spectra is to improve the signal-to-noise ratio (S/N). The common coadding methods are median merging and mean (sum) merging. The advantage of median is that it can effectively remove the cosmic rays, but the disadvantage is that the S/N is lower than the mean measurement. Mean merging gives a narrower (less noisy) distribution than merging by median, though both substantially reduced the width of the distribution. The conclusion so far is that combining by averaging is mildly preferable to combining by median. Computationally, the mean is also faster to compute than the median.

In our pipeline, we used mean merging method. The wavelengths of the three single exposure spectra are firstly aligned. Then the positions of the cosmic rays are determined by using the 3σ method and are replaced with the maximum value at this position in the other two spectra. After testing, the cosmic rays can be removed effectively with this method. Finally, the three spectra without cosmic rays are directly summed together. The results are shown in the Figure 3. As can be seen from Figure 3, the cosmic rays are removed completely and the S/N ratio has been significantly improved.

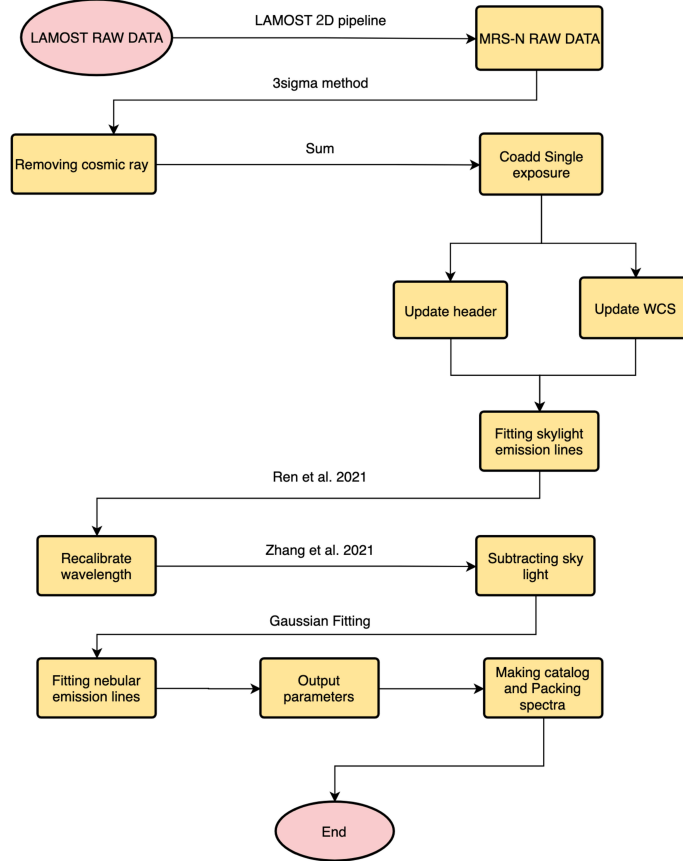


Fig. 2 The *MRS-N Pipeline* flowchart.

3.2 Wavelength recalibration

The sky light emission lines, which are mostly from the Meinel rotation-vibration bands of OH (Meinel, 1950), are ubiquitous in spectra of stars, galaxies or nebulae (Osterbrock & Martel, 1992; Osterbrock et al., 1996); they usually exhibit rich emission lines and a weak continuum in the optical spectra. The fainter the observed objects, the more serious the sky light lines contaminate its spectra. Therefore, in nebular spectra, the sky light emission lines appear particularly prominent. Because of its narrow spectral line width and fixed central wavelength, it can be well used as comparison lines to correct the wavelength zero point of spectra.

The raw data of MRS-N is wavelengths calibrated with calibration lamp but without subtracting sky light and correcting flat field. However, the lamp spectra and scientific spectra aren't observed at the same time, which means that the instrument status may have changed. Therefore, strictly speaking, it

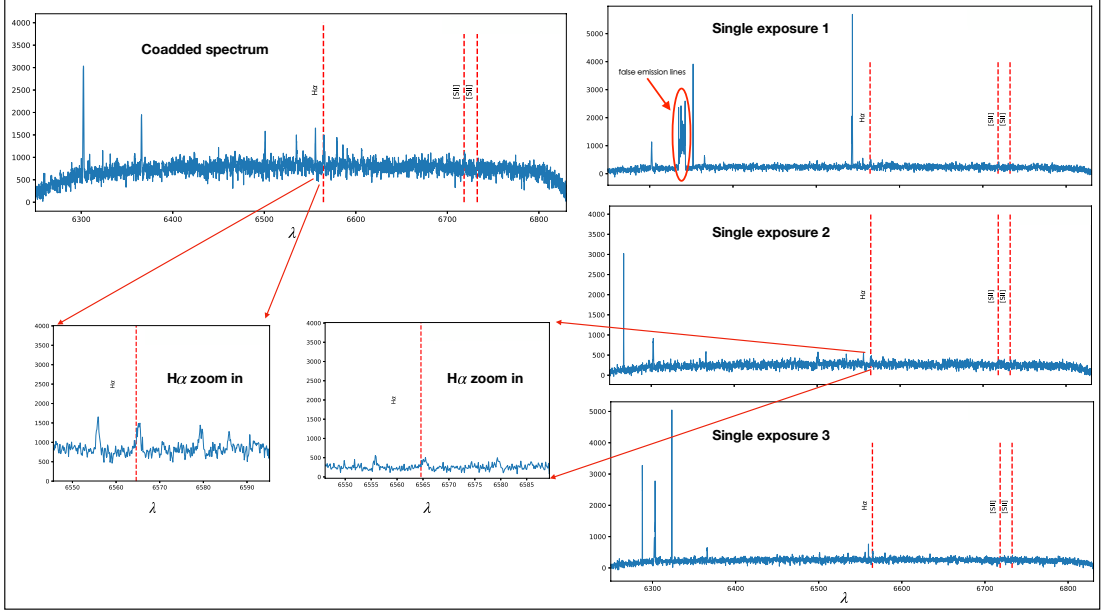


Fig.3 Comparison of coadded spectrum and single exposure. From the two graphs in the lower left corner, it is clear that the S/N of coadded H α is improved significantly. The red dotted lines in each panel represent nebular emission lines. It shows that the false emission lines in Single exposure 1 (red ellipse) has been completely eliminated.

will introduce instrument errors when doing calibration with lamp spectra. This problem can be perfectly solved when the scientific spectra are calibrated with skylight emission lines. Take the red band spectrum of MRS-N as an example, Figure 4 shows a spectrum with the night sky emission lines and nebular emission lines. These sky light emission lines and nebular lines are observed at the same time under the same instrument status. The central wavelengths of the sky light emission lines in scientific spectra are the same as the theoretical value. So, by fitting the sky light emission lines, we can obtain the relationship between the central wavelengths of sky light lines and the wavelength of the MRS-N spectra. With this relationship, the scientific spectrum can be recalibrated. Ren et al. (2021) provided a calibration function ($f(\lambda) = a\lambda^2 + b\lambda + c$, λ is the wavelength in unit of μm , a , b and c are the three indexes fitted with sky light lines) by using this method to correct the RVs of scientific spectra in real time. The accuracy of RVs could be improved to less than 1km s^{-1} .

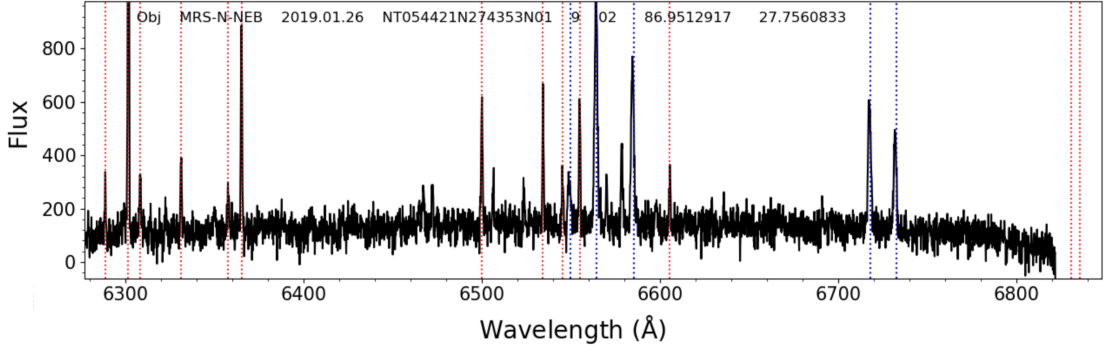


Fig. 4 An example spectrum (red band) of MRS-N with many skylight lines (red dotted lines) and nebular emission lines (blue dotted lines).

3.3 Subtracting Sky Light

Sky light subtraction is necessary for the ground-based spectrograph. The traditional method (Soto et al., 2016) of removing sky light is not suitable for MRS-N data. Zhang et al. (2021) introduced a method of subtracting sky light for spectra of MRS-N base on the relation of $I(H\alpha_{\text{sky}})/I(\lambda 6554)$ and solar altitude, which is the angle of the sun relative to the Earth's horizon. $I(\lambda 6554)$ is the flux of the OH at 6554Å which is from the Earth's atmosphere. Zhang et al. (2021) concluded that $I(H\alpha_{\text{sky}})/I(\lambda 6554)$ and solar altitude have the following relationship:

$$I(H\alpha_{\text{sky}})/I(\lambda 6554) = 0.954 - 0.011 \times (-\text{Sunalt})$$

So, Once the altitude of the observed target is known, the ratio of $I(H\alpha_{\text{sky}})/I(\lambda 6554)$ can be obtained. We can calculate the $I(\lambda 6554)$ by single Gaussian fitting. The $I(H\alpha_{\text{sky}})$ can be constructed with three parameters of Gauss function: the line centroid (μ), line dispersion (σ) and line intensity (I). Where $\mu_{H\alpha_{\text{sky}}} = 6563/6554 \times \text{RV}(\lambda 6554)$, $\sigma_{H\alpha_{\text{sky}}} = \sqrt{\sigma(\lambda 6554)^2 + 0.02^2}$ Å, and $I(H\alpha_{\text{sky}}) = \text{ratio} \times I(\lambda 6554)$, where $\text{ratio} = 0.954 - 0.011 \times (-\text{Sunalt})$. Then the constructed $I(H\alpha_{\text{sky}})$ is subtracted from the MRS-N spectra. By using this method, 90% of the sky light mixed in nebular $H\alpha$ emission lines can be reduced, which significantly improves the accuracy of nebulae classification and the measurements of nebular physical parameters. Figure 5 shows the results of before (left panel) and after (right panel) subtracting sky light. In the left panel of Figure 5, the red curve represents the Gaussian fitting of $H\alpha$ before subtracting sky light, blue curve represents the Gaussian fitting of sky light. In the right panel of Figure 5, the red curve represents the Gaussian fitting of $H\alpha$ after subtracting sky light.

3.4 Measurements of Nebular Parameters

All the physical parameters, such as RVs, full width at half maximum (FWHM), line intensity, etc., are measured by the Gaussian fitting method, which is widely utilized in spectra of the Sloan Digital Sky Survey (SDSS) (Rebassa-Mansergas et al., 2016) and LAMOST spectra (Ren et al., 2018a). We first fit all the science spectra with a second-order polynomial plus a single-Gaussian line profile. According to the χ^2 and fitting error, the spectra with larger χ^2 value and fitting error will be fitted again by the method of a second-order polynomial plus a double/triple-Gaussian line profile (Ren et al., 2021). Figure 6 shows three examples of the single-Gaussian fitting results of $H\alpha$, [N II] and [S II] emission lines which are from one MRS-N nebular spectrum.

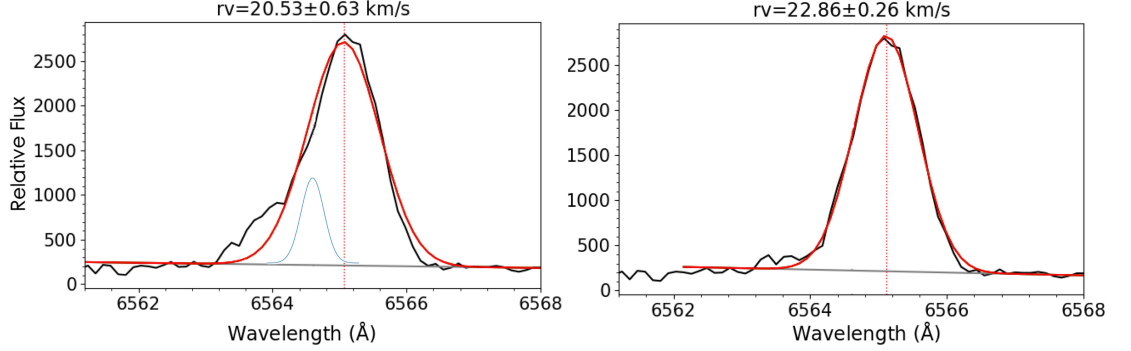


Fig. 5 Comparison of before and after subtracting sky light. *left panel*: Red curve represents the Gaussian fitting of H α before subtracting sky light, blue curve represents the Gaussian fitting of sky light. *right panel*: Red line represents the Gaussian fitting of H α after subtracting sky light. The red dotted lines in the two panels show the centroids of nebular H α emission line.

4 DATA PRODUCTS

Until now, more than 190 thousands nebular spectra have been observed in MRS-N. The data processing is in progress. The data products generated by the *MRS-N Pipeline* contains the following:

Nebular Spectra: The single exposure spectra and coadded spectra are all stored in *fits* format. They are all wavelength-recalibrated and sky-subtracted spectra. In these spectra, there are no spectra of stars. The stellar spectra observed in MRS-N will be processed by LAMOST 2D and 1D pipeline or LSP3. Since there are fewer nebular emission lines at the blue band of MRS (Wu et al., 2021), these spectral data are mainly for the red band, which covers the wavelength range 6300Å - 6800Å with $R \sim 7500$. The *fits* files of single exposure spectra are named in the form of **spec-XXr-PID-YYYYMMDD-N.fits**, where **XX** represents the spectrograph number (between 01 and 16), **PID** is the name of observed plate, **YYYYMMDD** shows the date of observation, **N** indicates the number (between 01 and 03) of single exposure. The structure of a single exposure spectrum is the same as the structure of LAMOST raw data (See http://dr1.lamost.org/doc/data-production-description#toc_3).

The names of coadded spectra are in the form of **sumspec-XXr-PID-YYYYMMDD.fits**. The string **XX**, **PID** and **YYYYMMDD** have the same meanings as above. Figure 7 shows the structure of a coadded spectrum. From Figure 7, we can see that each *fits* file has four extensions (EXTEN0, EXTEN1, EXTEN2 and EXTEN3). EXTEN0, EXTEN1 and EXTEN3 represent the relative flux, recalibrated wavelength and invert variance (Luo et al., 2015) of EXTEN0, respectively. EXTEN2 shows the informations of observed targets. Each extension includes 250 rows, indicating the spectral data of 250 fibers mounted on every spectrograph.

Nebular Parameters Catalog: The catalogs of nebular parameters are also stored in *fits* format. Each catalog contains 41 columns. Table 1 shows the detailed description for each column.

5 SUMMARY

As one of the largest nebular spectra survey on the northern GP, LAMOST MRS-N has conducted for three years (since Oct. 2018) and accumulated more than 190 thousands medium-resolution nebular spectra. In order to make it easier for users to understand and use data, we developed the *MRS-N Pipeline* for the reduction of MRS-N data. The *MRS-N Pipeline* should be used in combination with

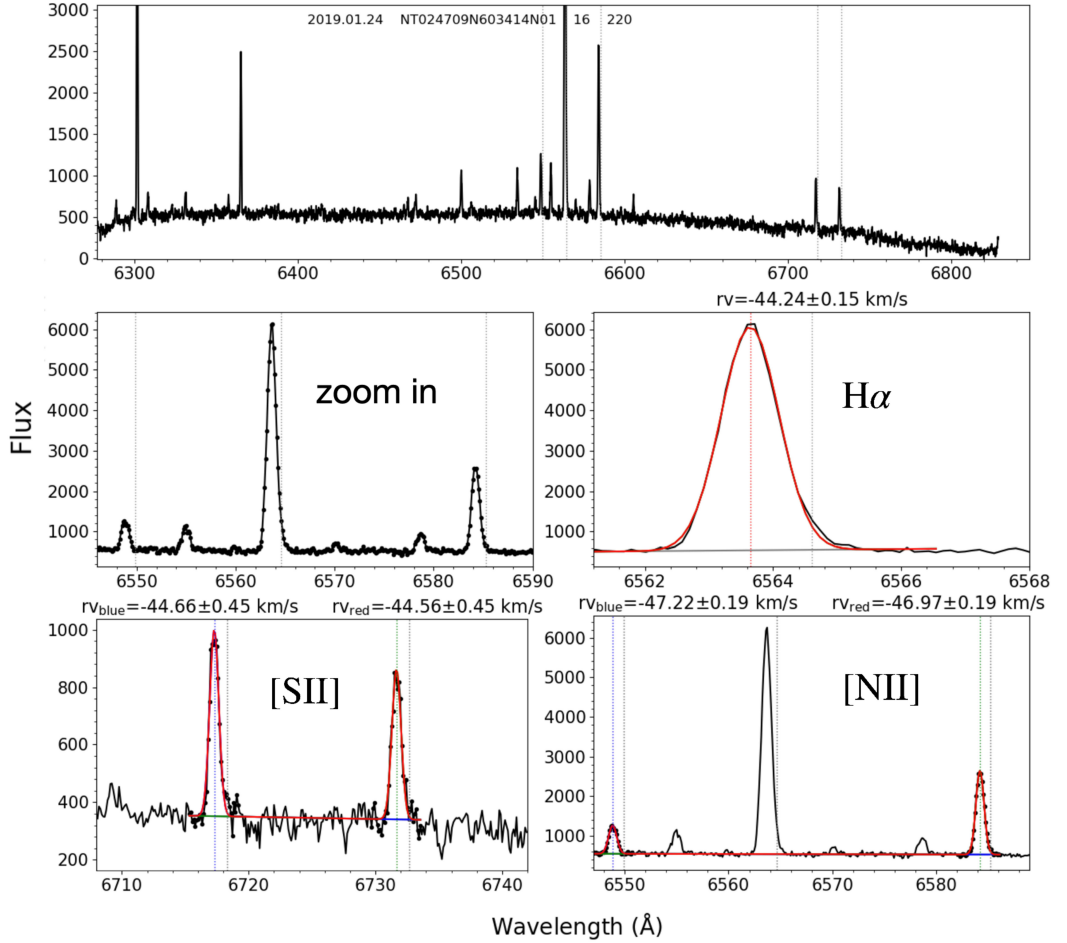


Fig. 6 The Gaussian fitting of three nebular emission lines. All the nebular paramers are from the fitting results.

Index	Extension	Type	Dimension	View				
<input type="checkbox"/> 0	Primary	Image	5000 × 250	Header	Image	Table		
<input type="checkbox"/> 1	NoName	Image	5000 × 250	Header	Image	Table		
<input type="checkbox"/> 2	NoName	Binary	38 cols × 250 rows	Header	Hist	Plot	All	Select
<input type="checkbox"/> 3	NoName	Image	5000 × 250	Header	Image	Table		

Fig. 7 The structure of a coadded spectrum.

LAMOST 2D Pipeline. It mainly includes removing cosmic rays, merging single exposure, fitting sky light emission lines, subtracting skylight, wavelength recalibration, meauring nebular parameters, creating catalogs and packing spectra. In addition, to improve the utilization of fibers, the fiber without coordinates can alsos be recalibrated. By using the *MRS-N Pipeline*, the accuracy of nebulae classification and the measurements of nebular physical parameters can be significantly improved.

Acknowledgements This project is supported by the National Natural Science Foundation of China (Grant Nos. 12073051, 12090041, 12090040, 11733006, 11403061, 11903048, U1631131, 11973060, 12090044, 12073039, 11633009, U1531118), and the Key Laboratory of Optical Astronomy, National Astronomical Observatories, Chinese Academy of Sciences, and the Key Research Program of Frontier Sciences, CAS (Grant No. QYZDY-SSW- SLH007).

C.-H. Hsia acknowledges the supports from the Science and Technology Development Fund, Macau SAR (file No. 0007/2019/A) and Faculty Research Grants of the Macau University of Science and Technology (No. FRG- 19-004-SSI).

Guoshoujing Telescope (the Large Sky Area Multi-Object Fiber Spectroscopic Telescope LAMOST) is a National Major Scientific Project built by the Chinese Academy of Sciences. Funding for the project has been provided by the National Development and Reform Commission. LAMOST is operated and managed by the National Astronomical Observatories, Chinese Academy of Sciences

References

- Cui, X.-Q., Zhao, Y.-H., Chu, Y.-Q., et al. 2012, *Research in Astronomy and Astrophysics*, 12, 1197
- Gao, S., Liu, C., Zhang, X., et al. 2014, *ApJ*, 788, L37
- Gu, W.-M., Mu, H.-J., Fu, J.-B., et al. 2019, *ApJ*, 872, L20
- Huang, Y., Liu, X. W., Yuan, H. B., et al. 2016, *MNRAS*, 463, 2623
- Huang, Y., Zhang, H. W., Wang, C., et al. 2019, *ApJ*, 884, L7
- Karoff, C., Knudsen, M. F., De Cat, P., et al. 2016, *Nature Communications*, 7, 11058
- Li, H., Tan, K., & Zhao, G. 2018, *ApJS*, 238, 16
- Li, J., FELLOW, L., Liu, C., et al. 2019, *ApJ*, 874, 138
- Liu, C. 2019, *MNRAS*, 490, 550
- Liu, C., Fang, M., Wu, Y., et al. 2015, *ApJ*, 807, 4
- Liu, C., Xu, Y., Wan, J.-C., et al. 2017a, *Research in Astronomy and Astrophysics*, 17, 096
- Liu, C., Wang, Y.-G., Shen, J., et al. 2017b, *ApJ*, 835, L18
- Liu, C., Fu, J., Shi, J., et al. 2020, *arXiv e-prints*, arXiv:2005.07210
- Liu, J., Zhang, H., Howard, A. W., et al. 2019, *Nature*, 575, 618
- Luo, A. L., Zhang, H.-T., Zhao, Y.-H., et al. 2012, *Research in Astronomy and Astrophysics*, 12, 1243
- Luo, A. L., Zhao, Y.-H., Zhao, G., et al. 2015, *Research in Astronomy and Astrophysics*, 15, 1095
- Luo, Y.-P., N  meth, P., Liu, C., Deng, L.-C., & Han, Z.-W. 2016, *ApJ*, 818, 202
- Meinel, I. A. B. 1950, *ApJ*, 111, 555
- Osterbrock, D. E., Fulbright, J. P., Martel, A. R., et al. 1996, *PASP*, 108, 277
- Osterbrock, D. E., & Martel, A. 1992, *PASP*, 104, 76
- Rebassa-Mansergas, A., Ren, J. J., Parsons, S. G., et al. 2016, *MNRAS*, 458, 3808
- Ren, J. J., Rebassa-Mansergas, A., Parsons, S. G., et al. 2018a, *MNRAS*, 477, 4641
- Ren, J.-J., Liu, X.-W., Chen, B.-Q., et al. 2018b, *Research in Astronomy and Astrophysics*, 18, 111
- Ren, J.-J., Wu, H., Wu, C.-J., et al. 2021, *Research in Astronomy and Astrophysics*, 21, 051
- Shen, S.-Y., Argudo-Fern  ndez, M., Chen, L., et al. 2016, *Research in Astronomy and Astrophysics*, 16, 43
- Soto, K. T., Lilly, S. J., Bacon, R., Richard, J., & Conseil, S. 2016, *MNRAS*, 458, 3210
- Su, D.-Q., & Cui, X.-Q. 2004, *ChJAA (Chin. J. Astron. Astrophys.)*, 4, 1
- Tian, H.-J., Liu, C., Wu, Y., Xiang, M.-S., & Zhang, Y. 2018, *ApJ*, 865, L19
- Tian, H.-J., Liu, C., Carlin, J. L., et al. 2015, *ApJ*, 809, 145
- Tian, H.-J., Liu, C., Wan, J.-C., et al. 2017, *Research in Astronomy and Astrophysics*, 17, 114
- Tian, H., Liu, C., Xu, Y., & Xue, X. 2019, *ApJ*, 871, 184
- Wang, C., Liu, X. W., Xiang, M. S., et al. 2019a, *MNRAS*, 482, 2189
- Wang, C., Huang, Y., Yuan, H. B., et al. 2019b, *ApJ*, 877, L7
- Wang, H.-F., Liu, C., Xu, Y., Wan, J.-C., & Deng, L. 2018, *MNRAS*, 478, 3367
- Wang, Q., Wang, Y., Liu, C., Mao, S., & Long, R. J. 2017a, *MNRAS*, 470, 2949
- Wang, S., Bai, Y., Zhang, C.-P., & Liu, J.-F. 2017b, *Research in Astronomy and Astrophysics*, 17, 10

- Wang, S.-G., Su, D.-Q., Chu, Y.-Q., Cui, X., & Wang, Y.-N. 1996, *Appl. Opt.*, 35, 5155
- Wu, C.-J., Wu, H., Liu, K., et al. 2016, *Research in Astronomy and Astrophysics*, 16, 102
- Wu, C.-J., Wu, H., Hsia, C.-H., et al. 2020, *Research in Astronomy and Astrophysics*, 20, 033
- Wu, C.-J., Wu, H., Zhang, W., et al. 2021, *Research in Astronomy and Astrophysics (RAA)*, 21, 96
- Wu, X.-B., Chen, Z.-Y., Jia, Z.-D., et al. 2010a, *Research in Astronomy and Astrophysics*, 10, 737
- Wu, X.-B., Jia, Z.-D., Chen, Z.-Y., et al. 2010b, *Research in Astronomy and Astrophysics*, 10, 745
- Xiang, M.-S., Liu, X.-W., Yuan, H.-B., et al. 2015a, *Research in Astronomy and Astrophysics*, 15, 1209
- Xiang, M. S., Liu, X. W., Yuan, H. B., et al. 2015b, *MNRAS*, 448, 822
- Xu, Y., Liu, C., Xue, X.-X., et al. 2018, *MNRAS*, 473, 1244
- Yu, J., & Liu, C. 2018, *MNRAS*, 475, 1093
- Zhang, W., Wu, H., Wu, C., et al. 2021, *arXiv e-prints*, arXiv:2108.08021
- Zhao, G., Zhao, Y.-H., Chu, Y.-Q., Jing, Y.-P., & Deng, L.-C. 2012, *Research in Astronomy and Astrophysics*, 12, 723
- Zhao, J. K., Zhao, G., Aoki, W., et al. 2018, *ApJ*, 868, 105

Table 1: The description of MRS-N parameters catalog

Name of each column	Description
obsdate	Date of observation
plate	The name of observed region
sp	The number of spectrograph
fiber	The number of fiber in each spectrograph
fibertype	Fiber type of target, such as Obj, Sky, F-std, Unused, PosErr, Dead
objtype	Object type from input catalog, such as Nebula, Skyline, F-star, Star...
RA	Fiber pointing Right Ascension (J2000), in degrees
DEC	Fiber pointing Declination (J2000), in degrees
SN _{Hα}	S/N of H α
SN _[N II] _[N6548]	S/N of [N II] at 6548Å
SN _[N II] _[N6584]	S/N of [N II] at 6584Å
SN _[S II] _[S6717]	S/N of [S II] at 6717Å
SN _[S II] _[S6731]	S/N of [S II] at 6731Å
RV _{Hα}	Heliocentric RVs of H α
errRV _{Hα}	Uncertainty of RVs for H α
RV _[N II]	Heliocentric RVs of [N II]
errRV _[N II]	Uncertainty of RVs for [N II]
RV _[S II]	Heliocentric RVs of [S II]
errRV _[S II]	Uncertainty of RVS for [S II]
$\lambda_{H\alpha}$	Fitted line centroid of H α
err $\lambda_{H\alpha}$	Uncertainty of fitted line centroid for H α
$\lambda_{[N II]}$ _[N6548]	Fitted line centroid of [N II] at 6548Å
err $\lambda_{[N II]}$ _[N6548]	Uncertainty of fitted line centroid for [N II] at 6548Å
$\lambda_{[N II]}$ _[N6584]	Fitted line centroid of [N II] at 6584Å
err $\lambda_{[N II]}$ _[N6584]	Uncertainty of fitted line centroid for [N II] at 6584Å
$\lambda_{[S II]}$ _[S6717]	Fitted line centroid of [S II] at 6717Å
err $\lambda_{[S II]}$ _[S6717]	Uncertainty of fitted line centroid for [S II] at 6717Å
$\lambda_{[S II]}$ _[S6731]	Fitted line centroid of [S II] at 6731Å
err $\lambda_{[S II]}$ _[S6731]	Uncertainty of fitted line centroid for [S II] at 6731Å
F _{Hα}	Line intensity of H α
errF _{Hα}	Uncertainty of line intensity for H α
F _[N II] _[N6548]	Line intensity of [N II] at 6548Å
errF _[N II] _[N6548]	Uncertainty of line intensity for [N II] at 6548Å
F _[N II] _[N6584]	Line intensity of [N II] at 6584Å
errF _[N II] _[N6584]	Uncertainty of line intensity for [N II] at 6584Å
F _[S II] _[S6717]	Line intensity of [S II] at 6717Å
errF _[S II] _[S6717]	Uncertainty of line intensity for [S II] at 6717Å
F _[S II] _[S6731]	Line intensity of [S II] at 6731Å
errF _[S II] _[S6731]	Uncertainty of line intensity for [S II] at 6731Å
FWHM _{Hα}	Fitted FWHM of H α
errFWHM _{Hα}	Uncertainty of fitted FWHM for H α
FWHM _[N II] _[N6548]	Fitted FWHM of [N II] at 6548Å
errFWHM _[N II] _[N6548]	Uncertainty of fitted FWHM for [N II] at 6548Å
FWHM _[N II] _[N6584]	Fitted FWHM of [N II] at 6584Å
errFWHM _[N II] _[N6584]	Uncertainty of fitted FWHM for [N II] at 6584Å

$\text{FWHM}_{[\text{S II}]}_{6717}$	Fitted FWHM of [S II] at 6717 Å
$\text{errFWHM}_{[\text{S II}]}_{6717}$	Uncertainty of fitted FWHM for [S II] at 6717 Å
$\text{FWHM}_{[\text{S II}]}_{6731}$	Fitted FWHM of [S II] at 6731 Å
$\text{errFWHM}_{[\text{S II}]}_{6731}$	Uncertainty of fitted FWHM for [S II] at 6731 Å
